Journal of Cultural Heritage 50 (2021) 13–24

Contents lists available at ScienceDirect

Journal of Cultural Heritage

journal homepage: www.elsevier.com/locate/culher

Assessment of preservation coatings for fiber-cement panels used in XX century mural paintings in Mexico

Nora A. Pérez[a,§,*], Isabel López-Arvizu[b,§], Adrián Mejía-González[c,§], Pablo Aguilar-Rodríguez[c,§], Nuria Esturau-Escofet[c,§,*], Daniel Meléndez[b,1], Erik Pérez-Ramírez[d], Sandra Ramírez[e]

[a] CONACYT-Instituto de Investigaciones Estéticas, Universidad Nacional Autónoma de México, Circuito Mario de la Cueva s/n, Ciudad Universitaria, Ciudad de México. C.P. 04510, México
[b] Instituto de Investigaciones Estéticas, Universidad Nacional Autónoma de México, Circuito Mario de la Cueva s/n, Ciudad Universitaria, Ciudad de México, C.P 04510, México
[c] Instituto de Química, Universidad Nacional Autónoma de México, Circuito exterior s/n, Ciudad Universitaria, Ciudad de México, C.P 04510, México
[d] Escuela Nacional Preparatoria - Plantel 8 Miguel E. Schultz, Av. Lomas de Plateros s/n, Universidad Nacional Autónoma de México, Ciudad de México, C.P 01600, México
[e] Centro Nacional Conservación y Registro del Patrimonio Artístico Mueble, del Instituto Nacional de Bellas Artes y Literatura, San Ildefonso 60, Cuauhtémoc, Ciudad de México, C.P 06000, México

ARTICLE INFO

Article history:
Received 12 October 2020
Accepted 7 June 2021
Available online 3 July 2021

Keywords:
Polymer coatings, fiber-cement panel
Mural painting
Artificial weathering
Nmr spectroscopy
physical tests

ABSTRACT

In Mexico, fiber-cement panels (FCP) were widely used by mural artists to create monumental works in the 1950s and 1960s. The durability of heritage structures made with concrete and cement is a concern nowadays, especially for those reinforced with asbestos fibers. As it was discovered in the second half of the 20th century, asbestos fibers represent a considerable health risk if inhaled. It is therefore relevant to analyze different conservation strategies such as industrial coating materials. In the present research, we analyze before and after an artificial weathering process the behavior of three polymer coatings applied on FCP to reduce the disintegration of its surface: Acrylic resin (AR), Polyurethane resin (PUR) and Alkyd enamel (AE). The methodology proposed was designed both by restorers and heritage scientists to provide comprehensive results that considered the specificity of heritage conservation. The chemical characterization of coatings by NMR combined with FTIR-ATR gives a detailed structure description. The change on physical properties and surface morphology after the weathering was related to the chemical composition of these coating materials. The results indicate that after the accelerated weathering exposure, the polymer coatings did not suffer chemical degradation, but the weathering conditions compromised the film formation process of the PUR causing physical transformations that can subsequently affect the FCP. For the AE and AR color and water absorption were the most affected properties respectively. This detailed investigation offers an understanding of the behavior of different polymer coatings on fiber-cement mural paintings, which can provide guidance of the materials to be used for conservation purposes.

© 2021 Elsevier Masson SAS. All rights reserved.

1. Introduction

In recent years, various types of coatings have been designed and applied for preservation of cultural heritage materials, such as wood, metal, stone and masonry, but the durability of cement and concrete heritage as the one used in modern art paintings is a recent issue that needs to be tackled. In industrial applications, surface coatings have a significant role in the protection and preservation of structures. It is however unclear, if these industrial surface coatings are suitable for conservation purposes [1,2].

Fiber-cement panels (FCP) are building materials that have been used in construction for over 100 years. The Czech engineer, Lud-

* Corresponding authors.
E-mail addresses: norari.perez@gmail.com (N.A. Pérez), amejiag@iquimica.unam.mx (A. Mejía-González), pablo.aguilar@iquimica.unam.mx (P. Aguilar-Rodríguez), nesturau@iquimica.unam.mx (N. Esturau-Escofet), erik.perez@enp.unam.mx (E. Pérez-Ramírez), srmunoz@inba.gob.mx (S. Ramírez).
§ Participants from Laboratorio Nacional de Ciencias para la Investigación y la Conservación del Patrimonio Cultural (LANCIC, National Science Laboratory for Research and Conservation of Cultural Heritage)
[1] Present address: Coordinación Nacional de Conservación del Patrimonio Cultural, Instituto Nacional de Antropología e Historia, General Anaya S/N, San Diego Churubusco, Coyoacán, Ciudad de México, C.P 04120, México

https://doi.org/10.1016/j.culher.2021.06.006
1296-2074/© 2021 Elsevier Masson SAS. All rights reserved.

wik Hatschek invented and patented the technology for manufacturing a light and durable asbestos cement sheet that he called "Eternit". This fiber-cement composite showed improved toughness, ductility, flexural capacity, and crack resistance. Even though the improved properties, the degradation of the composite eventually causes a loss of cohesion of the cement matrix which provokes the asbestos fibers to disperse in the surrounding area. After being discovered that asbestos are carcinogenic, a global effort to remove asbestos from construction materials started in the 1970s [3].

In Mexico, fiber-cement was widely used by artists, as it was considered an economical material that allowed the creation of transportable works. The Hotel Casino de la Selva (1931–2002) in Cuernavaca, Morelos stored a vast number of works based on asbestos-reinforced-cement panels. This famous building belonged to Manuel Suárez y Suárez, a renowned Spanish businessman in the construction materials industry, including fiber-cement, who also became one of the most important patrons of Mexican muralism. Other notable works on FCP made by muralists between the 1950s and 1960s are *Human creation and the economy* (1963) by Benito Messeguer at the NarcisoBassols Auditorium of the UNAM School of Economics, the paintings at the Polyforum Cultural Siqueiros by David Alfaro Siqueiros both at Mexico City, *Apatzingán Congress* (1964) by Roberto Cueva del Río located in the Municipal Palace of Cuernavaca, Morelos, *El amor* (1967) by Silvio Benedetto at the Autonomous University from Chilpancingo, Guerrero, *The Man as Creator* (1968) by Lorenzo Guerrero Ponce, and *From agriculture to industry: The land dominating man, Man dominating the earth, Man Fruit of the Earth and Electronic Prometheus* (1969) by Mario Orozco Rivera at the Agricultural Bank of Culiacán, Sinaloa, among several others [4].

Mural paintings that use FCP as support suffer from cement matrix degradation and consequently, from asbestos fiber dispersion as stated above. This effect has been observed only in the back part of the mural since the pictorial layer applied in the front by the artist acts like a coating. The release of asbestos is the first concern due to the risk it represents to the painting itself, but also for human health. Once the support panel has started to loose cohesion, other deterioration effects appear such as water filtration and biodeterioration [5]. Due to the need to maintain the cohesion of the cement-matrix to prevent water transport inside the FCP from the back towards the front paint layer and considering the observed preventive conservation function of the pictorial layer, the application of a specific protective coating on the back part of the paintings' support is considered a suitable conservation option.

Coatings are a thin synthetic polymer-based material applied to the concrete's surface to protect it from damage and are designed to provide adequate resistance to the environment in which they are applied. As such, they need long-term monitoring of their properties since the polymers' mass swells and eventually disintegrates with time. These materials can protect and slow down the concrete's rate of deterioration. Coatings performance is a complex function that depends on the material type, formulation, thickness, surface preparation and adhesion. Commercially available examples of materials used as coatings are based on acrylic, epoxy, siloxane and organosilane polymers. [6–9].

Due to the large amount of modern architecture that withholds murals painted on FCP in Mexico and the inevitable degradation that they may suffer or in many cases are already suffering, a multidisciplinary study of the materials that can be used for the preservation of the paintings, in addition to prevent the release of asbestos fibers, is considered relevant.

2. Research aim

To evaluate before and after an artificial weathering process the physical, chemical, and surface properties of different polymer coatings applied on FCP specimens.

3. Materials and methods

The methodology includes a physical evaluation designed by conservators considering this assessment usually is done on a scaffolding for mural paintings. Subsequently, an instrumental characterization was carried out by conservation scientists.

3.1. Materials

The pictorial technique of David Alfaro Siqueiros in his 1964–1967 period was selected to be reproduced in test specimens, as there are outdoor murals from this period that are currently the target for future restoration treatments. His-murals from this period are made of acrylic paint applied on FCP joined to a metal frame by iron screws [5]. The red acrylic paint (RAP) Carmine Red 319 from Politec®, a waterborne material reported to be used by David Alfaro Siqueiros was selected to simulate the pictorial layer on the test specimens.

The coatings selection was made considering the following criteria: i) previously applied coatings for conservation of modern paintings, ii) industry recommended coatings for encapsulating asbestos fibers and, iii) affordable price for the conservation institutions in Mexico. The selected coatings were:

- Acrylic resin Colorcel Eternit® (AR): A waterborne material, with a matte beige color, is reported to have aggregates and biocides in its formulation. While the product vendor indicates it is designed for protecting fiber-cement materials, it can also be applied to concrete walls, bricks and masonry. The supplier indicates a one-layer application.
- Polyurethane resin Barniz11000® (PUR): A solvent-based transparent material suitable for application on cement materials as well as other porous substrates. The PUR is a two-component formulation of monomer (PUR/M) and catalyst (PUR/C). The PUR/M and PUR/C were mixed in a 3:1 ratio. Once the PUR mix was prepared the application consisted in two stages as indicated by the vendor datasheet: first, the PUR mix was dissolved at 50%v/v in polyurethane solvent and two layers were applied, this is called the basecoat; second, the PUR mix was dissolved at 30%v/v in the same solvent and then three layers were applied, this is called the finishcoat. Therefore, a total of five layers were applied of the same nature but in different concentrations.
- Alkyd enamel NovoPermo® Básico (AE): A solvent-based material with a semi-matte gray color, prepared in a 2 to 1 ratio of enamel to mineral spirit (paint thinner). This coating is not specific nor for asbestos or cement but has been previously employed for conservation of modern mural paintings in Mexico. The supplier indicates a one-layer application.

3.2. Specimen's preparation

The front of a fiber-cement panel was painted with the RAP to perform in the specimen as the pictorial layer. 20 specimens of 30 cm x 15 cm (5 replicates for each coating and 5 replicates of

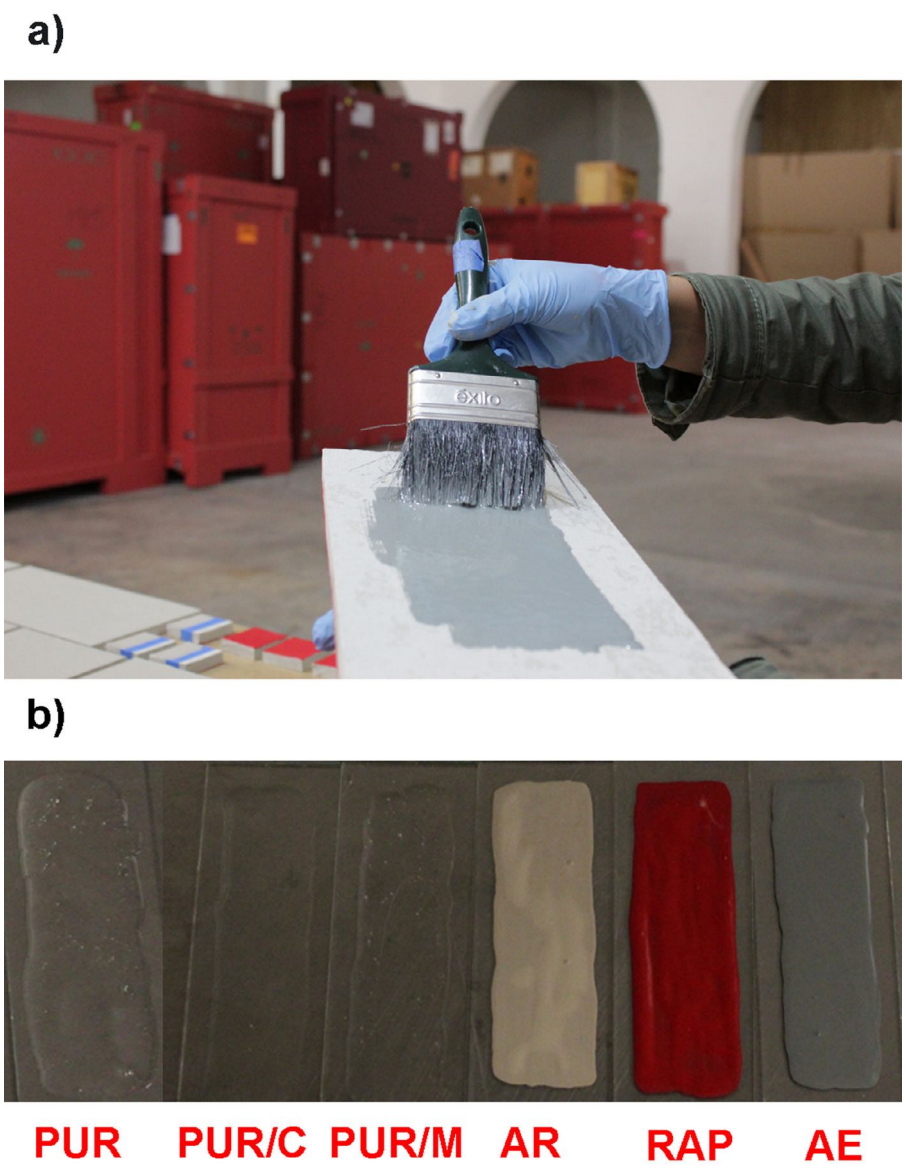

Fig. 1. Preparation of the specimens for the experiment. a) Fiber-cement panels, b) Glass slides references.

Table 1
Summary of coating properties during application.

Coating type	Number of components	Number of layers	Ease of application / layer homogeneity	Drying time / min	Coverage / m^2L^{-1}	Finish	Texture
AR	1	1	good / good	5	5	matte	same
PUR	2	2 basecoat/3 finishcoat	medium / good	3/10/6/8/11	5	glossy	as FCP
AE	1	1	medium / good	125	2.5	glossy	

a non-coated FCP) were cut from the painted panel following the Mexican standard for handling hazardous materials [10]. The protective coatings were applied in the reverse of the panels with a thick paintbrush, as it would be on site for the artwork (Fig. 1a). During the specimen preparation, the temperature (20 °C) and the relative humidity (47–52%) were registered with a data logger. The subsequent properties were registered as a qualitative way to assess the operational process of coatings application:

- Layer homogeneity: abundance of lump formation.
- Ease of application: fluidity of the material from the brush to the panel.
- Drying time: time for the surface to be dry to touch.
- Paint yield: volume of material required by m^2 of panel.
- Matte or glossy finish: determined by observation in comparison with the coating specifications.

Each coating was also applied on glass slides as reference specimens (Fig. 1b). After 15 days of the application both test and reference specimens were subjected to artificial weathering conditions.

3.2.1. Artificial weathering

The artificial weathering protocol considered heat and moisture as variables, since these parameters can affect both polymeric and cement materials [11–13]. ASTM standard C1442 [14] was modified to fit the devices available in the laboratory, the 20 specimens

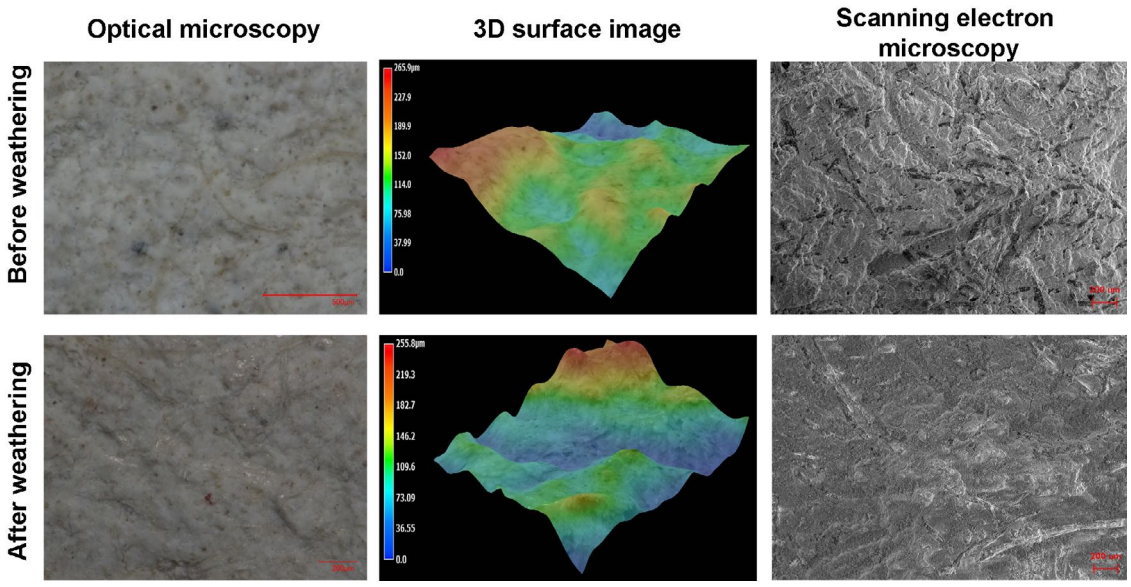

Fig. 2. Microscopic examination of the FCP surface before and after weathering.

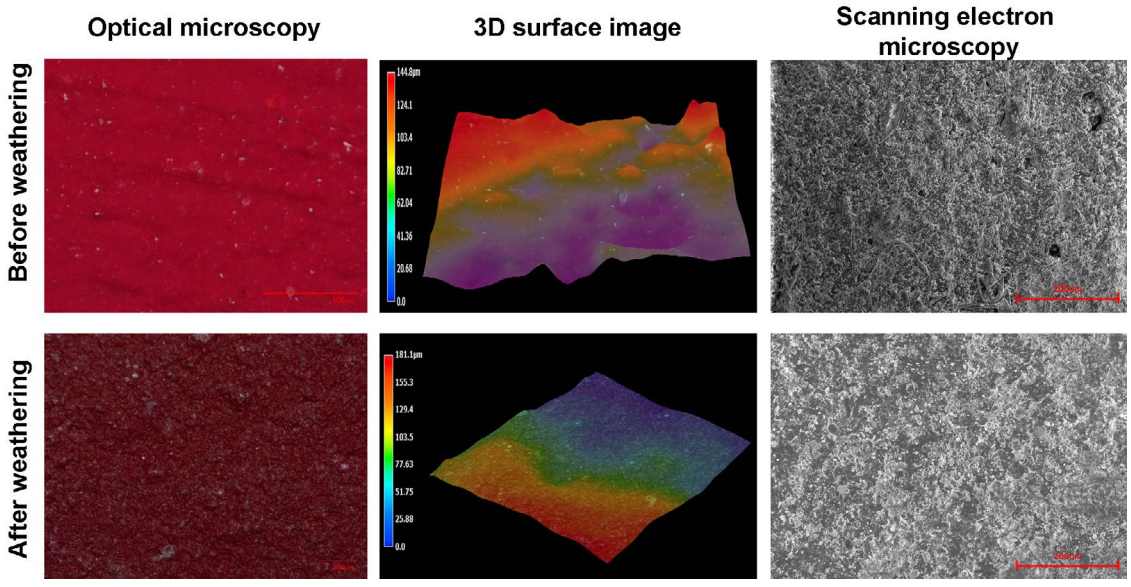

Fig. 3. Microscopic examination of the RAP surface before and after weathering.

were sprayed with purified water until completely moisten, then they were placed under the shadow to dry for 120 min. This treatment comprises one wetting-drying cycle. Afterwards, the specimens went into a convection oven at temperature of 50 ± 20 °C for 20 h and then 2 h cooling with the oven off. This treatment comprises one heating-cooling cycle. A total of 56 wetting-drying and heating-cooling cycles (1344 h) were completed to ensure that not only the coatings, but also the FCP suffered some degree of weathering [13,15].

3.3. Physical tests

For comparing the specimens' physical properties against the original FCP, on site measurement methods often applied by conservators were employed: The surface color was evaluated with the Munsell color chart in order to determine visual changes, the hydrophobic behavior was tested with the water drop test timing the loss of contact angle and scratch resistance was tested by comparison with the Mohs scale. For complementary purposes, additional color measurements were carried out using a NCS-RUBY spectrometer (STIL) with a tungsten halogen light source and a spot of 0.5 cm diameter. The data was analyzed by considering the CIELab color system and the total color change before and after weathering was calculated by the following equation defined by the CIE (*Commission Internationale de L'Eclaraige*) [16].

$$\Delta E*_{ab} = \left[(\Delta L*)^2 + (\Delta a*)^2 + (\Delta b*)^2\right]^{1/2} \quad (1)$$

3.4. Microscopic examination

3.4.1. Optical microscopy (OM)

The morphology of the coated surfaces was assessed with a Keyence VHX2000E microscope, micrographs and 3D surface models were obtained at various amplifications.

3.4.2. Scanning electron microscopy (SEM)

The surface micromorphology and the measurement of the layer thickness were carried out on small samples from the speci-

Table 2
Measured physical properties before and after artificial weathering.

	FCP		RAP	
	before	**after**	**before**	**after**
Color (Munsell code)	5Y 8/1	10YR 8/1	7.5R 4/16	10R 3/10
Color change (ΔE^*_{ab})	1.1		0.8	
Drop absorption time (average)	0 s	46 s	2 min	30 min
Mohs hardness	3	3	3	3

	AR COATING		PUR COATING		AE COATING	
	before	**after**	**before**	**after**	**before**	**after**
Color (Munsell code)	10YR 8/1	10YR 7/1	7.5Y 7/2	7.5Y7/4	10BG 6/1	10GY 6/1
Color change (ΔE^*_{ab})	2.0		4.4		19.1	
Drop absorption time (average)	0 s	19 min	25 min	12 min	25 min	23 min
Layer thickness (µm)	60-120	30-50	2-5	1-4	9-36	10-20
Mohs hardness	5	4	4	4	4	4

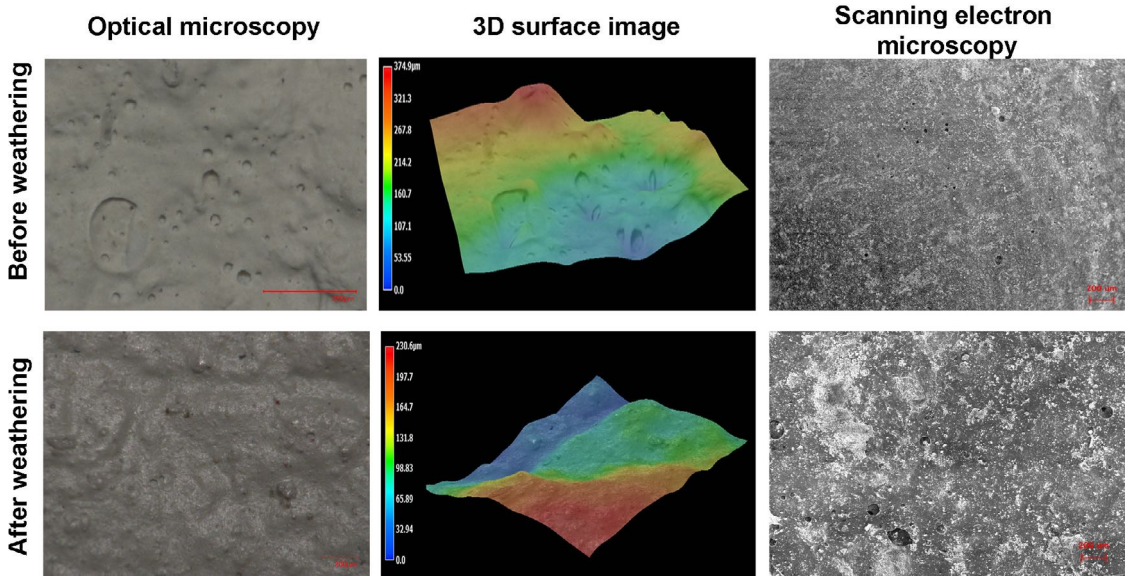

Fig. 4. Microscopic examination of the AR coating surface before and after weathering.

mens. Surface and cross-section samples of the coatings were observed in a Zeiss EVOMA25 scanning electron microscope in secondary electron mode at 15 kV with variable pressure conditions.

3.5. Chemical characterization

In order to characterize the coatings and to correlate the changes of the measured physical properties and surface morphology to the chemical composition, a set of analytical techniques were employed on the specimens before (both fresh and dried/cured state) and after the weathering process.

3.5.1. Infrared spectroscopy (FTIR)

Infrared spectroscopy was performed in a Bruker ALPHA spectrometer in Total Attenuated Reflectance (ATR) mode, with 32 scans and a 4000–400 cm^{-1} range. The resolution of the equipment is 2 cm^{-1}.

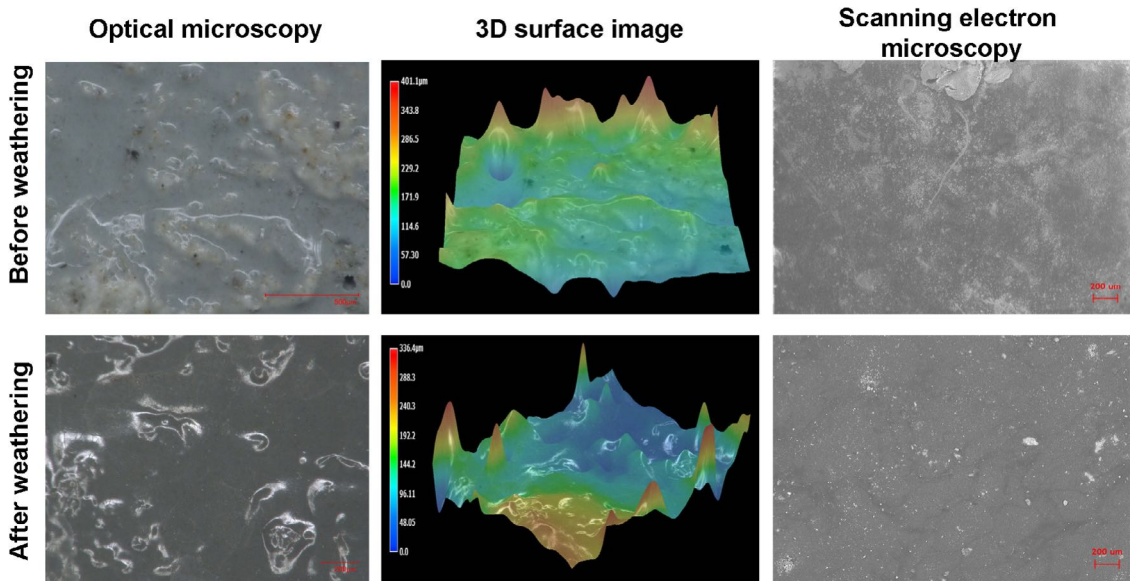

Fig. 5. Microscopic examination of the AE coating surface before and after weathering.

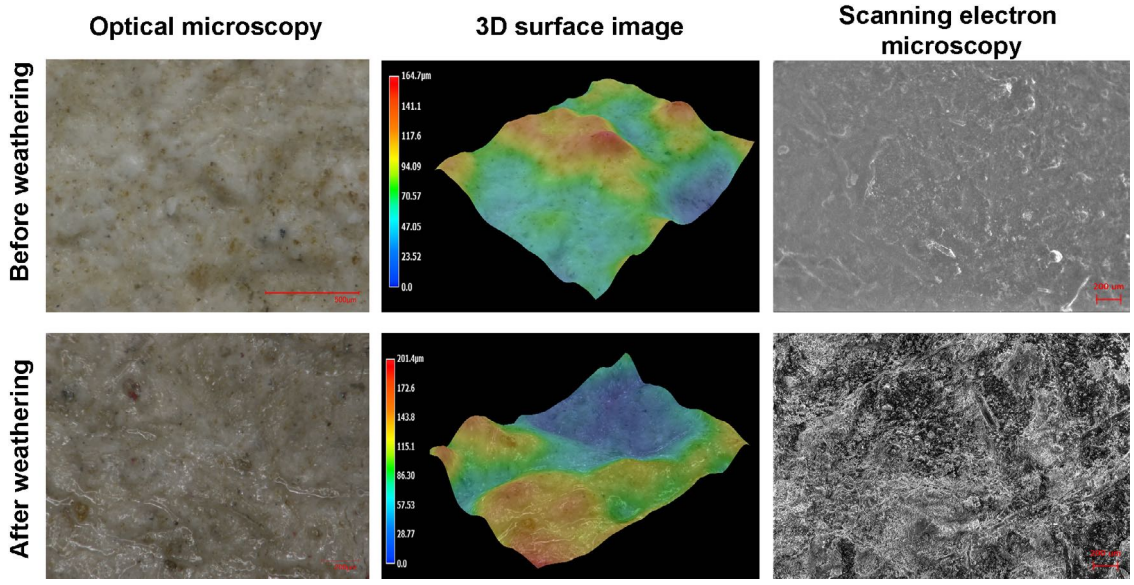

Fig. 6. Microscopic examination of the PUR coating surface before and after weathering.

3.5.2. Nuclear magnetic resonance (NMR)

Nuclear Magnetic Resonance spectra were acquired on a Bruker Avance III HD 700 spectrometer (operating at ^{1}H nominal frequency of 700 MHz) equipped with a 5 mm z axis gradient TCI cryoprobe. AR, AE and RAP samples were dissolved in deuterated chloroform ($CDCl_3$) and the PUR samples in dimethyl sulfoxide ($DMSO–d_6$), at 25 °C. ^{1}H NMR, ^{13}C NMR and the 2D-NMR experiments: edited heteronuclear single quantum correlation spectroscopy (edited-HSQC) and heteronuclear multiple-bond correlation spectroscopy (HMBC) from $^{1}H–^{13}C$ and $^{1}H-^{15}N$. The ^{1}H NMR and ^{13}C NMR spectra were referenced to the residual signals of the solvents: 7.26 and 77.0 ppm for $CDCl_3$, and 2.50 and 39.50 ppm for $DMSO–d_6$.

3.5.3. Direct analysis in real time mass spectrometry (DART-MS)

Mass spectra were acquired using a JMST100LC Accu TOF mass spectrometer (JEOL, Japan) with DART ion source in positive mode at 19.8 eV and low resolution.

4. Results

The observations of the coatings properties showed the importance of the application method on the results of the experimentation (Table 1). The roughness of the fiber-cement promoted good adhesion of the first applied coating layers, the adhesion of subsequent layers of PUR depended on the material itself, but it was observed that the FCP texture was still helpful.

During the application, the fluidity of the materials was related to the layer homogeneity. The lump formation on the surface was considered as one parameter. The lumps can be defined as crystallized polymer particles that usually take place during the manufacturing of the material and can be made visible in liquid or solid state; the lumps are also associated with the powder additives in the mixture [17]. The AR was found to have an intermediate fluidity, which was attributed to the components included in the formulation. The AE and PUR presented high fluidity which caused

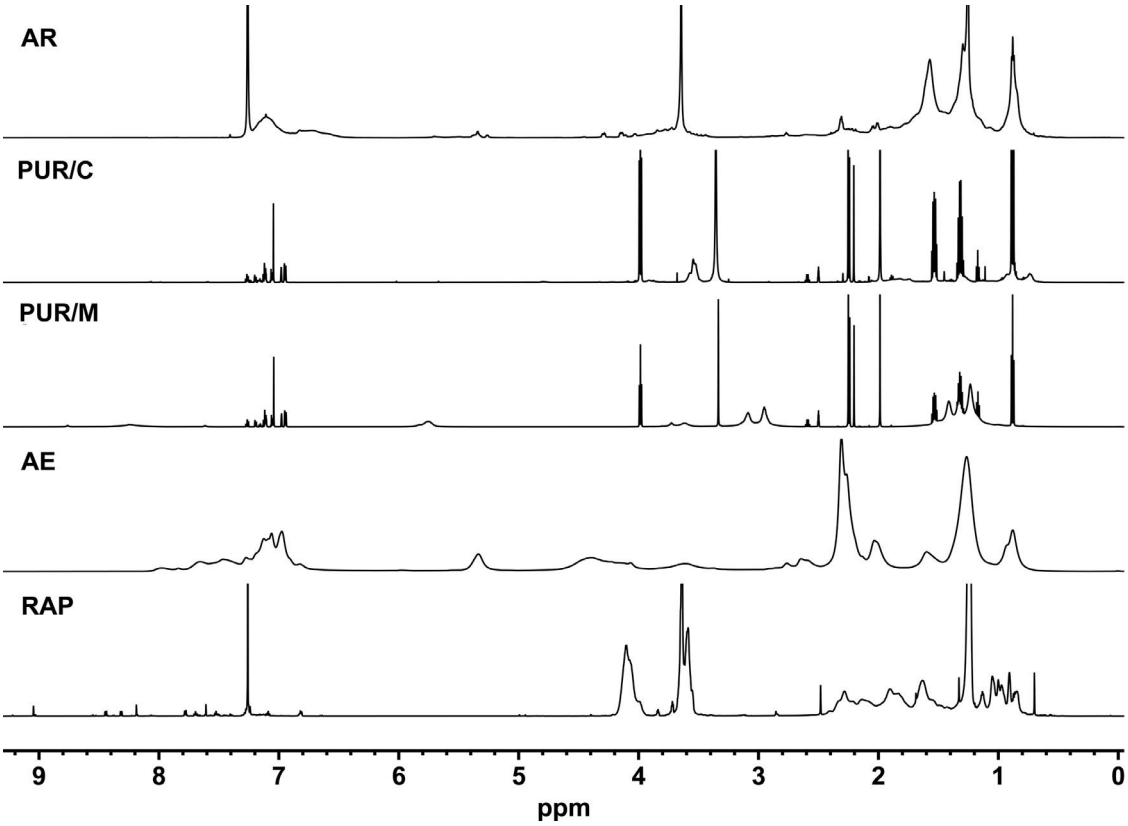

Fig. 7. ^{1}H NMR spectra (700 MHz, $CDCl_3$) of AR, PUR/C, PUR/M, AE and RAP samples (arbitrary units on the Y-axis).

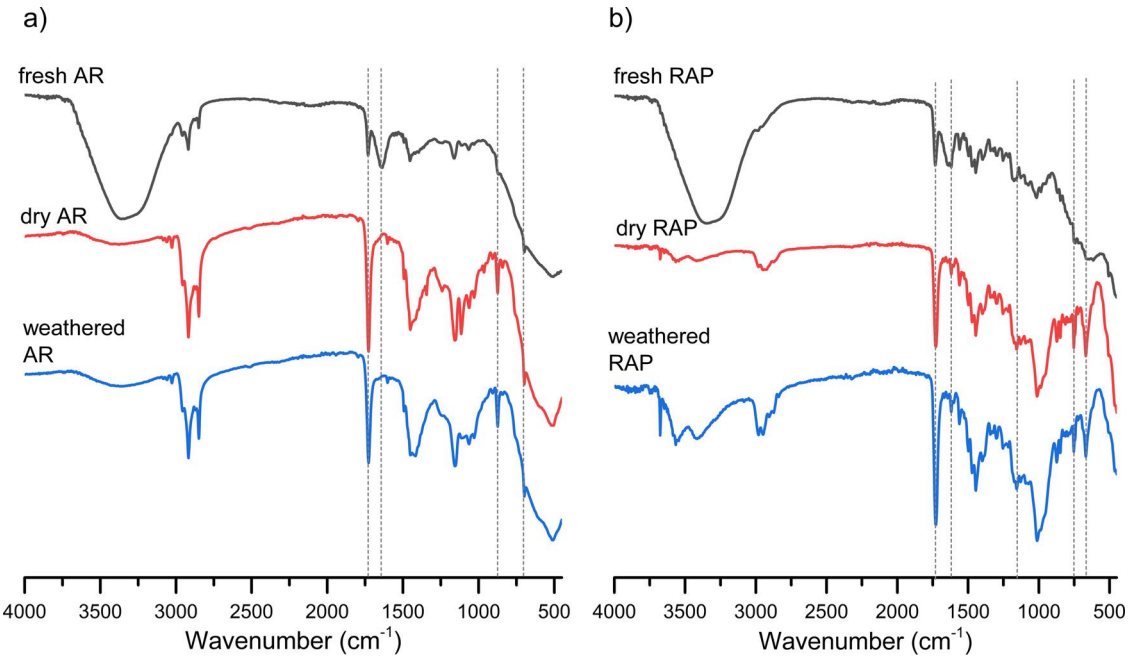

Fig. 8. Infrared ATR spectra comparison of the fresh, dry and weathered a) AR coating b) RAP (arbitrary units on the Y-axis).

spills over the support edges. All three coatings had layers without lumps or accumulations of material.

The AR layer dried by evaporation of water and was the easiest, fastest coating to prepare and apply. The first PUR layer had the fastest drying time (3 min) due to the chemical reaction between the two components and quick solvent evaporation, while the slowest PUR layer took up to 11 min. Despite the quick drying of the PUR layers, this material had the longest application time (about 278 min), as the manufacturer recommends a four-hour drying period between the basecoat and finishcoat. The AE had the longest drying time (more than 2 h) due to a slow solvent's evaporation.

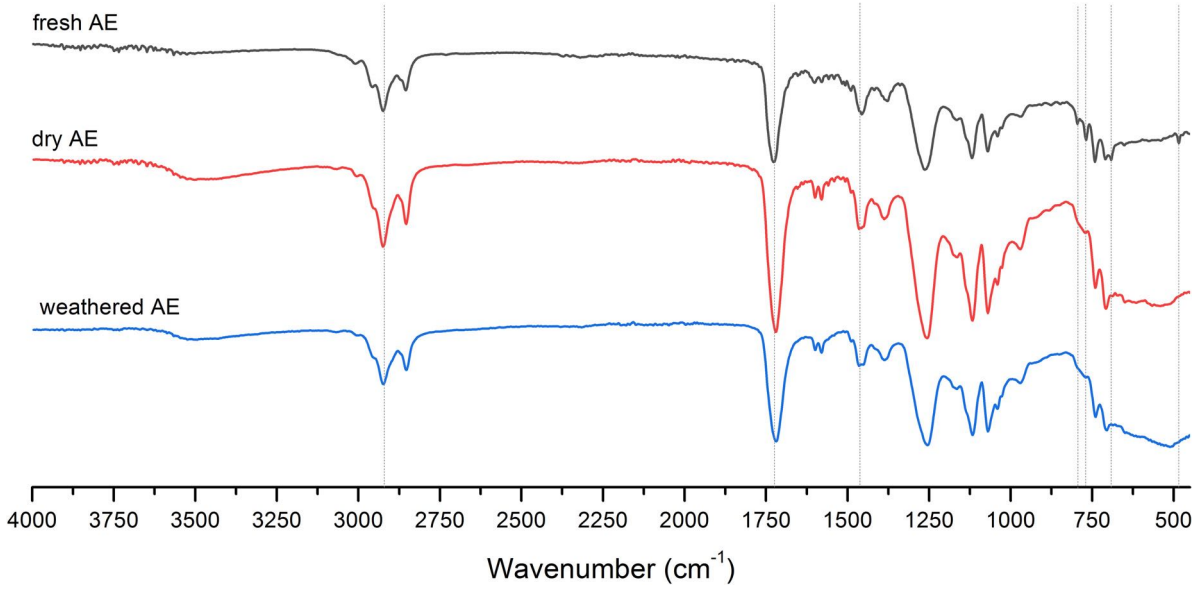

Fig. 9. Infrared ATR spectra comparison of the fresh, dry, and weathered AE coating (arbitrary units on the Y-axis).

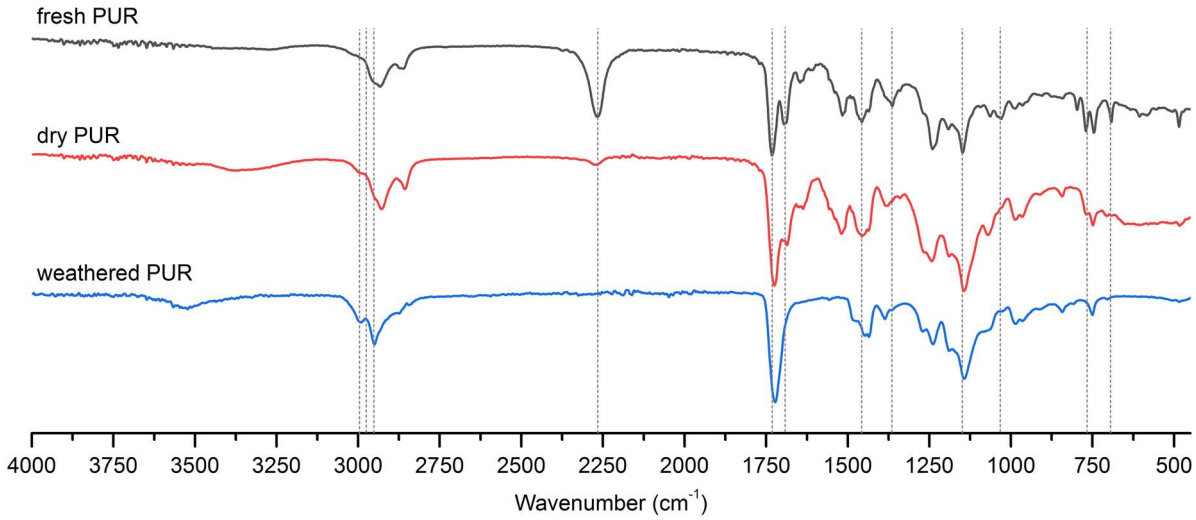

Fig. 10. Infrared ATR spectra comparison of the fresh, dry and weathered PUR coating (arbitrary units on the Y-axis).

4.1. Physical tests

All the physical properties measurements on the FCP and RAP, as well on the coatings before and after their artificial weathering are summarized in Table 2. These include color, water absorption and hardness data.

4.1.1. Color measurement

The color change of the FCP when the treatment was applied showed that the AR coating provided the lowest modification with a $\Delta E^*_{ab} = 4.7$, while the PUR and the AE coatings had a ΔE^*_{ab} of 9.7 and 11.5 respectively.

Once the materials were aged, the FCP and the RAP showed the lowest color change ($\Delta E^*_{ab} \leq 1.1$). The AR coating had a slight color modification ($\Delta E^*_{ab} = 2.0$), and the PUR and AE coatings turned to yellow values, with ΔE^*_{ab} of 4.4 and 19.1 respectively. These results agree with the observations made with the Munsell system.

4.1.2. Water absorption

The FCP surface was highly hydrophilic and immediately absorbed the drop of water. Nevertheless, after weathering this behavior changed due to the superficial roughness and the alteration of the cement matrix, which left the asbestos fibers- which are naturally hydrophobic- exposed, increasing the drop of water absorption time. The RAP also significantly incremented the drop of water absorption time after weathering.

Before weathering, all the freshly applied coatings were impermeable. However, AR coating increased its hydrophobicity significantly after weathering. On the contrary, the PUR coating became more hydrophilic, but it was still impermeable to water in comparison to the uncoated FCP, while AE coated samples had a hydrophobic behavior which did not change noticeably despite the weathering procedure.

4.1.3. Mohs hardness measurements

The scratch resistance of the panel was increased after the coatings' application and remained so after weathering. Only AR coating showed a decrease from 5 to 4 in the Mohs scale after weathering.

4.2. Microscopic examination

4.2.1. Fiber-Cement panel (FCP)

The distribution of the fibers and the cement matrix was observed on the microscopic images (Fig, 2). Before weathering, the fibers were within the cement as showed by the OM and SEM images. After weathering, the 3D surface image showed more peaks and pits, evidencing that some fibers were partially exposed. These surface changes indicate an initial degradation of the FCP cement matrix.

4.2.2. Red acrylic paint (RAP)

The RAP microscopic analysis (Fig. 3) showed that the paint layer covered the FCP texture. The peaks and surface waviness observed before the weathering in the 3D image are associated with the application method given that the brush strokes are clearly observed in the OM image. The SEM images show the morphology of the FCP fibers. After weathering, the surface roughness changed and the peaks and pits were no longer present. In the SEM scale, the aggregates became more apparent and the FCP fibers were no longer observed.

4.2.3. Acrylic resin (AR)

Microscopic examination (Fig. 4) showed that the AR coating formed surface bubbles of different sizes, therefore allowing the formation of pores. After weathering, the surface changed from a matte to a glossy finish, but no specific local roughness transformation was observed. The SEM images allowed to determine that the coating's aggregates formed agglomerations on the surface. Despite the pores observed before and after weathering on the coatings, the FCP fibers were never observed.

4.2.4. Alkyd enamel (AE)

AE coating microscopy images (Fig. 5) showed that the coating was not applied homogeneously, a fact attributed to the fluidity of the material. It had a translucent appearance that initially allowed the fiber-cement to be seen, but after aging a gloss change occurred. In the 3D images it was possible to observe the change in the waviness of the surface due to the weathering process. In the SEM images these morphological changes were still observed, including the separation of the aggregates on the surface which explains its new gloss after aging. The FCP texture was observed under the coating, but no cement degradation was observed.

4.2.5. Polyurethane resin (PUR)

Microscopic examination of the PUR coating (Fig. 6) showed that the FCP texture was preserved, but after weathering it thinned and a color change occurred. The sample became glossier and the waviness of the surface increased. The asbestos fibers' morphology was observed in the SEM images and after weathering the disaggregation of the cement matrix was observed. These results indicate that the PUR coating was permeable enough to allow de FCP alteration.

4.3. Chemical characterization before weathering

In the ^{1}H NMR spectra of each sample (Fig. 7), signals with different intensities and widths are observed, which implies that the samples are complex mixtures. The chemical structures of the main organic compounds were elucidated by means of 1D and 2D NMR experiments (S1). In the RAP sample, the presence of ethyl acrylate – methyl methacrylate copolymer poly(EA-co-MMA) as a binder was confirmed, as well as the use of Triton X-100 as a surfactant and PR3 (toluidine red) as pigment [18–20].

In the AR coating, the compounds identified were poly n–butyl acrylate poly(nBA), polyStyrene, triolein and the same Octyl phenol ethoxylate surfactant Triton X-100. For the PUR sample solubility tests were performed in order to select a deuterated solvent for NMR analysis. It was found that PUR is not soluble in $CHCl_3$, THF at room temperature nor in DMSO at 65 °C; this characteristic is due to the insoluble irreversible network formed during the curing process [21]. For this reason, the two components of the sample were analyzed separately as PUR/M and PUR/C (S3). The compounds identified in PUR/C were: 1,6-diisocyanatohexane isocyanurates, hexamethylene diisocyanate (HDI), uretidone, 1,3-bis(6-isocyanatohexyl)urea, and 1,3,5-tris(6-isocyanatohexyl)biuret. All their respective molecular weights were confirmed through DART-MS, even the molecular weight of the HDI as a cyclized trimer (S2). The PUR/M sample was identified as an acrylic mixture of methyl methacrylate (MMA) and hydroxyethylmethacrylate (HEMA) which is commonly dimerized with MMA poly(HEMA-co-MMA) [22], and the benzotriazole propyl 3-(3-(2H-benzo[*d*][1,2,3]triazol-2-yl)−5-(tert–butyl)−4-hydroxyphenyl) propanoate used as the UV protector [23]. In both PUR samples the solvents o-, m-, p- xylene isomers, n–butyl acetate and ethyl benzene, were identified. In the AE layer, a linoleic oil-based alkyd resin as found, as well as the same solvents identified in the PUR samples.

In the FTIR-ATR spectra of each sample, the main signals of the inorganic and the organic compounds were assigned based on the compounds previously identified by NMR (Table 3).

4.4. Chemical characterization after weathering

Considering it was not possible to solubilize the PUR and AE samples to be analyzed by NMR, the study of the chemical composition of the samples after weathering was carried out mainly by FTIR-ATR.

4.4.1. Acrylic materials (AR and RAP)

Spectra of the AR sample were analyzed in each of three stages: when the layer was fresh, after the drying process and after the weathering process (Fig. 8a). In the FTIR-ATR spectrum of the fresh sample, the broad bands observed at 3400–3250 cm^{-1} and 1635 cm^{-1} (υOH, H_2O) were related to the large amount of water which causes attenuation of the other signals. FTIR-ATR spectrum of the AR sample after the drying process shows the corresponding signals of the NMR identified components, and after the induced weathering a decrease was observed in the signals at 1343 cm^{-1} (δas C–H,-CH_2-), 1113 cm^{-1} (υC–O) and 964 cm^{-1} (C–O str.) that were related to the surfactant Triton X-100. In the case of the RAP samples (Fig. 8b), the same effect of the presence of water was observed, just as in the AR sample. In the dry and in the aged samples no apparent changes in signal intensity were observed. The weathered sample of this material was analyzed by ^{1}H NMR and it was confirmed that the surfactant Triton X-100 was the compound that was lost after aging process [18].

4.4.2. Alkyd enamel (AE)

The main difference on the FTIR-ATR spectra of the fresh, dry and weathered sample (Fig. 9) was the displacement of the $C=O$ signal from 1726 to 1716 cm^{-1} (υ $C=O$, sterified phtalic acid), this modification was related to the curing process which involved the formation of the alkyd polymer [37]. No apparent changes were observed in the region between 1644 and 655 cm^{-1} except for the loss of the signals at 795, 767 and 484 cm^{-1} (δ C–H, mono- or di-substituted aromatic) [38], that corresponds to the xylenes which were evaporated after the curing process.

4.4.3. Polyurethane material (PUR)

The PUR was studied as a mixture of PUR/C and PUR/M. The FTIR-ATR signals of the components identified (Table 3) were re-

Table 3
Infrared-ATR characteristic absorptions of the components identified in the coating materials.

Sample	υ / cm^{-1} and component assignation
AR	**poly(nBA)**: 2960, 1730, 1450, 1395, 1240, 1165, 1064, 943, 837, 750, 737 cm^{-1}[24]. **polystyrene**: 3025, 2922, 2850, 1601, 1492, 1449, 1246, 1026, 906, 696 cm^{-1}[25]. **Triton X-100:** 2890, 1343, 1113, 964 cm^{-1}[26]. **Calcite**: 1425, 875 cm^{-1}[27]. **Water**: 1635 cm^{-1} [28].
PUR/C	**1,6-diisocyanatohexane isocyanurates**: 2936, 2856, 2263, 1765, 1691, 1627, 1513, 1455, 1368, 1334, 1248, 1155, 1090, 1033, 865, 765, 730 cm^{-1}[29,30]. **n-butyl acetate**: 1738,1244, 1066, 1042, 1031 cm^{-1}. **Isomeric mixture of xylenes**: 795, 691, 484 cm^{-1}. **Ethyl benzene**: 746 cm^{-1} [31].
PUR/M	**poly(HEMA-co-MMA)**: 3380, 3000, 2950, 1728, 1732, 1483, 1456, 1448, 1389, 1238, 1192, 1146, 990, 967, 750 cm^{-1}[32]. **n-butyl acetate**: 2876, 1738, 1435, 1388, 1366, 1120, 1066, 1042, 1031, 951, 634, 607 cm^{-1}. **Isomeric mixture of xylenes**: 795, 769, 691, 484 cm^{-1}. **Ethylbenzene**: 1453, 746, 697 cm^{-1} [31].
AE	**Linoleic oil-based alkyd resin:** 3070, 3010, 2958, 2923, 2955, 1726, 1602, 1579, 1466, 1382, 1263, 1165, 1120, 1070, 741, 708 cm^{-1}[33–35]. **Isomeric mixture of xylenes**: 795, 769, 691, 484 cm^{-1} [31].
RAP	**poly(EA-co-MMA)**: 2981, 2952, 2925, 1725, 1454, 1384, 1147, 848, 754 cm^{-1}. **Toluidine Red:** 1619, 1562, 1498, 1253, 1128, 754 cm^{-1} [36]. **Talc**: 3675, 1010, 669, 449, 424 cm^{-1}. **Calcite**: 1411, 871, 711 cm^{-1}. **Silicates**: 1174, 1110, 813, 790, 711, 449 cm^{-1} [27].

lated to the signals in the fresh PUR. After the drying process (Fig. 10), the poly(HEMA-MMA) acrylic polyol signals at 1289,1192 and 1146 ($O = C$–O-C str.), 990 and 967 cm^{-1}(C–C skel. vib.) remain constant. A decrease of solvents and isocyanurates 2263 (NCO out-of-phase), 1691 (polyurea $C = O$ free stretch), 1368 (δ -CH_2), 1033 (C–C skel. str.), 765 (C–N skel. str.) cm^{-1} signals were observed, which indicate a simultaneous process of solvent evaporation and resin curing. After the drying process, there are still signals from isocyanate groups of isocyanurates which react with water during the weathering process to form amines and CO_2 that could be ejected out of the resin's surface. After the weathering process the acrylic polyol signals at 3000 (ν_a -CH_3) and 2950 (ν_a -CH_2) cm^{-1} apparently increase, however this is due to the attenuation of the solvent and isocyanurate ones at 2936 (ν_s -CH_2), 2856 (ν_a -CH_2), 2263, 1691, 1368, 1033 and 765 cm^{-1} that overlap with some polyol signals. Polyurethane characteristic signals at 2873 (ν_a -CH_2), 1720 (H-bond $C = O$ stretch), 1384 δ -C(CH_3) and 846 (ν_s C–N-C) were identified. Therefore, it could be inferred that the acrylic polyol does not suffer changes and that cross-linking and solvent evaporation processes have been completed during the weathering process.

5. Discussion

The evaluation of the physical, chemical and surface properties of three different polymer coatings applied in FCP before and after an artificial weathering process was performed. Initially, the non-coated FCP used as reference was highly hydrophilic and immediately absorbed the drop of water; after weathering the surface became less hydrophilic. A small color variation was also measured and observed. These changes were attributed to the disaggregation of the matrix which exposed the mineral aggregates and the asbestos fibers as observed in the microscopy images (Fig. 2). This conferred hydrophobic properties and a contribution to the overall color by the FCP constituents (Table 2). Therefore, the artificial weathering conditions initiated the degrading of the FCP as expected, and is consistent with the results reported by Enfedaque et al. [39] after wet-dry cycles that affected the mechanical properties of fiber reinforced cements.

The fluidity factor of the coatings registered during the application stage (Table 1) was determinant for the coatings' properties as evidenced in the microscopic examination. Acrylic materials (RAP and AR) had good coverage of the surface and no asbestos fibers were observed before or after the weathering, although the AR coating thinned after aging. These results confirmed the field observations that the pictorial layer acts as a protective coating preventing the release of the fibers.

Both the pictorial layer and the AR coating had a hydrophobic behavior after the weathering cycles. This can be explained because some acrylic materials have lower affinity for polar substances due to the loss of the surfactant component that was identified in the NMR analysis.

An important conservation criterion regarding architectural heritage is the water-surface interaction. In our study, the analysis of the pictorial layer and the coatings provided new valuable knowledge, given that in the mural painting, the paint, the coating and the FCP will act as a three layer system in which the FCP is in the middle. Then the water absorption property of the pictorial layer must be considered when selecting a coating material, for it will play an important role in the environmental interaction of the mural.

The color alteration for the acrylic materials after weathering is attributed to the agglomeration of the fillers, as the surfactant phase washed away and the inorganic materials became more apparent -as seen in the SEM images (Fig. 3 and Fig. 4)- whereas the polymer matrix was not chemically degraded. This is in agreement with high ΔE values ($\Delta E \geq 3$) reported for acrylics subjected to thermal and relative humidity treatments [40].

Blistering and pinholes were observed as result of physical degrading and polymer redistribution under the weathering conditions, since the acrylic films are sensitive to humidity. The physical transformation of acrylic materials is similar to the one found after 300 h of UV exposure by Mejía et al. [18]. Also agrees with the changes reported by Izzo et al. [40] and like the latter authors no significant chemical changes were reported after UV, thermal or humidity aging.

The AE coating formed thin layers with surface defects attributed to the application method, this affected the protective function of the coating because asbestos fibers were observed at a microscopic level after the aging. The hydrophobic behavior was maintained, and the layer thickness was not significantly affected, this agrees with the fact that no significant transformations were identified in the chemical characterization. However, the color changed dramatically, shifting to yellow and black with gloss alteration. Given that the polymer structure did not degrade, the visual changes are then attributed to the volatiles and shrinkage of the polymer, whereas absorption and desorption of moisture, as well as changes in temperature contribute to surface roughening and thus the reduction of gloss [41].

The PUR coating was fluid and formed thin layers, after aging the coating was thin enough to allow the observation of the asbestos fibers and a degraded cement matrix at the microscopic level. After weathering, the PUR became more hydrophilic, attributed to the layer thinning but it was still impermeable to water in comparison to the non-coated FCP. The measured color change indicated the coating turned to yellow coordinates as observed and registered with the Munsell cards. The gloss change can be attributed to physical aging caused by the penetration of water and subsequent blistering. The fact that the coating became yellower is in agreement with the results reported by Kim et al. and Bhar-

gava et al. [42,43] who attribute this to a decrease in free carbonyl in the polyurethane binder and a decrease at 1236 cm^{-1} and 1170 cm^{-1} in the FTIR spectrum as resulting from the overall film erosion that was also reported by Zhang [44].

Chemical characterization indicates that the PUR coating did not suffer degradation, but the weathering conditions compromised its film formation process and caused physical transformations. This is a compelling result since the technical datasheets indicated that climate exposure can take place seven days after drying, and in our study the coatings had been dried for fifteen days before the weathering exposure started. We found that the exposure to water and heat can compromise the crosslinking reaction in the PUR, therefore considerations regarding the season and the weather of the coating application must be addressed in a conservation project program [6].

In the case of all studied materials the sequence of events leading to coating's degradation occurred mainly via stress formation and surface degradation, leading in different degrees to gloss and color change, as well as increased permeability [41]. No coating showed chemical degrading of the polymer.

6. Conclusions

In this research, three protective coatings for conservation of FCP employed in modern mural painting were studied before and after an artificial weathering process. The main objective of the conservation of the murals is to prevent the cement degradation and release of asbestos fibers so it does not affect the mural stability and the visiting public.

Under the experimental conditions the non-coated FCP suffered cement-matrix disintegration and therefore initial fiber release. The study confirmed the restorer's observations that in the case of acrylic pictorial layers they act as a protective coating for the front part of the panel. The surfacing of the asbestos in the back of the FCP was only observed in the case of the PUR samples. This indicates that it was the most sensitive coating to the experimental weathering conditions, concluding that the PUR curing process in our case occurred in unfavorable weather conditions and compromised the protective properties of the material. The AR and the AE coatings showed physical aging, with color displaying the most dramatic change.

As expected, the commercial coatings investigated show quite complex formulations. All were chemically stable to the artificial weathering, but the physical degradation reaffirms the fact that coatings constitute a sacrificial protection which is affected by the environment. This remarks that the choice of coatings must be associated with the establishment of a maintenance routine as they must be renewed periodically.

It is well known that the coating application method is important for an adequate performance, a fact confirmed by our results. Nevertheless, we used the most affordable tool for any restorer to apply the coatings: a thick brush. Therefore, to delve into this topic future work will include the influence of application methods on the coating's performance.

Acknowledgments

Laboratorio de Restauración de Obra Mural del CENCROPAM-INBA. This study made use of UNAM's NMR lab: LURMN at IQ-UNAM, which is funded by CONACYT Mexico (Project 0224747) and UNAM. We thank Dr. Ma. del Carmen García González for training in the use of the AccuTOF-DART mass spectrometer. We thank Dr. Alejandro Mitrani for the technical assistance in the artificial weathering process and manuscript reviewing.

Funding sources

This work was supported by the Laboratorio Nacional de Ciencias para la Investigación y Conservación del Patrimonio Cultural LANCIC under grants funding CONACYT LN279740, LN293904, LN299076, LN314846 and LN315853.

N.A.P. would like to thank to program Cátedras CONACYT (No. 267). P.A-R. would like to thank Instituto de Química UNAM and PAPIIT for his scholarships (grant IN402417). A.M.-G. would like to thank Consejo Nacional de Ciencia y Tecnología (CONACYT) for his scholarship (grant 846597).

Supplementary materials

Supplementary material associated with this article can be found, in the online version, at doi:10.1016/j.culher.2021.06.006.

References

[1] V. Horie, Materials For Conservation. Organic consolidants,Adhesives and Coatings, Second Ed., Butterworth-Heinemann, Oxford, 2010.
[2] R. Swamy, S. Tanikawa, Surface coatings to preserve concrete durability, in: R. Dhir, J. Green (Eds.), Prot. Concr., Taylor and Francis, London, 1990, pp. 129–144.
[3] K. Schabowicz, T. Gorzelańczyk, Z. Ranachowski, D. Jarząbek, The Fabrication, Testing and Application of Fibre Cement Boards, First Ed., Cambridge Scholars Publishing, Newcastle, 2018.
[4] O. Suárez, Inventario Del Muralismo mexicano. Siglo VII a. De C./1968, Instituto de Investigaciones Estéticas, Universidad Nacional Autónoma de México, Distrito Federal, 1972.
[5] Archive, CENCROPAM-INBA OF/D/SUB/CENCROPAM/298/2012, Mexico City, 2012.
[6] A. Wright, P. Kendall, The listening mirrors: a conservation approach to concrete repair techniques, J. Archit. Conserv. 14 (2008) 33–54.
[7] Z. Kamaitis, Structural design of polymer protective coatings for reinforced concrete structures. Part I: theoretical considerations, J. Civ. Eng. Manag. 13 (2007) 11–17.
[8] Z. Kamaitis, Structural design of polymer protective coatings for reinforced concrete structures. Part II: experimental verification, J. Civ. Eng. Manag. 13 (2007) 19–26.
[9] L.W. Teng, R. Huang, S.Y. Zou, H.M. Hsu, Protection effectiveness of concrete surface treating materials, Adv. Mater. Res. 834–836 (2013) 749–754.
[10] SEMARNAT, Official Mexican STANDARD NOM-052-SEMARNAT-2005 which establishes the characteristics, the identification procedure, classification and the lists of hazardous waste, Mexico, 2005.
[11] S. Michalski, Agents of Deterioration, 2009 https://www.canada.ca/en/conservation-institute/services/agents-deterioration.html.
[12] A. Peled, J. Jones, S.P. Shah, Effect of matrix modification on durability of glass fiber reinforced cement composites, Mater. Struct. Constr. 38 (2005) 163–171.
[13] R.L. Feller, Accelerated Aging. Photochemical and Thermal Aspects., The Getty Conservation Institute, Los Angeles, California, USA, 1994.
[14] ASTM International, ASTM C1442. Standard practice for conducting tests on sealants using artificial weathering apparatus, (2006).
[15] P. Sanmartín, F. Cappitelli, Evaluation of Accelerated Ageing Tests for Metallic and Non-metallic Grafitti Paints Applied to Stone, Coatings 7 (2017) 1–16.
[16] R.T. Marcus, The Measurement of Color, in: K. Nassau (Ed.), Color Sci. Art Technol, Elsevier Science B.V., 1998, pp. 31–96.
[17] E. Schweigger, Manual De Pinturas y Recubrimientos Plásticos, Ediciones Díaz de Santos, Madrid, 2005.
[18] A. Mejía-González, S. Zetina, M.E. Espinosa-Pesqueira, N. Esturau-Escofet, Characterization of commercial artists' acrylic paints and the influence of UV light on aging, Int. J. Polym. Anal. Charact. 22 (2017) 473–482.
[19] A. Ciccola, M. Guiso, F. Domenici, F. Sciubba, A. Bianco, Azo-pigments effect on UV degradation of contemporary art pictorial film: a FTIR-NMR combination study, Polym. Degrad. Stab. 140 (2017) 74–83.
[20] P. Aguilar-Rodríguez, A. Mejía-González, S. Zetina, A. Colin-Molina, B. Rodríguez-Molina, N. Esturau-Escofet, Unexpected behavior of commercial artists' acrylic paints under UVA artificial aging, Microchem. J. 160 (2021) 105743.
[21] S. Koltzenburg, M. Maskos, O. Nuyken, Polymer Chemistry, Springer-Verlag, Berlin, 2017.
[22] M. Szycher, Szycher's Handbook of Polyurethanes ed., CRC Press, 2012.
[23] P. Fromentin, T. Lertwattanaseri, Blue light cutting optical material comprising a benzotriazole UV absorber, EP3203271A1, 2017. https://register.epo.org/application?number=EP16305149&lng=en&tab=main.
[24] A. Kawasaki, J. Furukawa, T. Tsuruta, G. Wasai, T. Makimoto, Infrared spectra of poly(butyl acrylates), Die Makromol. Chemie. 49 (1961) 76–111.
[25] V.M. Zolotarev, Comparison of polystyrene IR spectra obtained by the T, R, ATR, and DR methods, Opt. Spectrosc. 122 (2017) 749–756.
[26] B. Ormsby, K. Elina, C. Miliani, T. Learner, An FTIR-based exploration of the effects of wet cleaning treatments on artists' acrylic emulsion paint films, E-Preservation Sci 6 (2009) 186–195.

[27] N.V. Chukanov, A.D. Chervonnyi, Infrared Spectroscopy of Minerals and Related Compounds, 1st ed., Springer International Publishing, Cham, 2016.
[28] D. Coker, J. Reimers, R. Watts, The Infrared Absorption Spectrum of Water, Aust. J. Phys. 35 (1982) 623–638.
[29] C. Defeyt, J. Langenbacher, R. Rivenc, Polyurethane coatings used in twentieth century outdoor painted sculptures. Part I: comparative study of various systems by means of ATR-FTIR spectroscopy, Herit. Sci. 5 (2017) 1–11.
[30] A.M. Kaminski, M.W. Urban, Interfacial studies of crosslinked polyurethanes; Part I. Quantitative and structural aspects of crosslinking near film-air and film-substrate interfaces in solvent-borne polyurethanes, J. Coatings Technol. 69 (1997) 55–66.
[31] S. Matsuyama, S. Kinugasa, K. Tanabe, T. Tamura, Spectral Database for Organic Compounds, National Institute of Advanced Industrial Science and Technology, 2020 (n.d.) https://sdbs.db.aist.go.jp accessed September 12.
[32] T.S. Perova, J.K. Vij, H. Xu, Fourier transform infrared study of poly (2-hydroxyethyl methacrylate) PHEMA, Colloid Polym. Sci. 275 (1997) 323–332.
[33] M.T. Doménech-Carbó, A. Doménech-Carbó, J.V. Gimeno-Adelantado, F. Bosch-Reig, Identification of Synthetic Resins Used in Works of Art by Fourier Transform Infrared Spectroscopy, Appl. Spectrosc. 55 (2001) 1590–1602.
[34] P.A. Hayes, S. Vahur, I. Leito, ATR-FTIR spectroscopy and quantitative multivariate analysis of paints and coating materials, Spectrochim. Acta Part A Mol. Biomol. Spectrosc. 133 (2014) 207–213.
[35] R. Ploeger, D. Scalarone, O. Chiantore, The characterization of commercial artists' alkyd paints, J. Cult. Herit. 9 (2008) 412–419.
[36] T.J.S. Learner, Analysis of Modern Paints, 1st ed., Getty Conservation Institute, Los Angeles, California, USA, 2004.
[37] U. Knuutinen, K. Paivi, Two case studies of unsaturated polyester composite art objects, E-Preservation Sci 3 (2006) 11–19.
[38] M. Lazzari, O. Chiantore, Drying and oxidative degradation of linseed oil, Polym. Degrad. Stab. 65 (1999) 303–313.
[39] A. Enfedaque, L.S. Paradela, V. Sánchez-Gálvez, An alternative methodology to predict aging effects on the mechanical properties of glass fiber reinforced cements (GRC), Constr. Build. Mater. 27 (2012) 425–431.
[40] F.C. Izzo, E. Balliana, F. Pinton, E. Zendri, A preliminary study of the composition of commercial oil, acrylic and vinyl paints and their behaviour after accelerated ageing conditions, Conserv. Sci. Cult. Herit. 14 (2014) 353–369.
[41] G. Wypych, Handbook of Material Weathering, Fifth Edit, ChemTec Publishing, Toronto, 2013.
[42] H. Kim, M.W. Urban, Molecular Level Chain Scission Mechanisms of Epoxy and Urethane Polymeric Films Exposed to UV /H 2 O, Multidimensional Spectroscopic Studies 57 (2000) 5382–5390.
[43] S. Bhargava, M. Kubota, R.D. Lewis, S.G. Advani, A.K. Prasad, J.M. Deitzel, Ultraviolet, water, and thermal aging studies of a waterborne polyurethane elastomer-based high reflectivity coating, Prog. Org. Coatings. 79 (2015) 75–82.
[44] Y. Zhang, J. Maxted, A. Barber, C. Lowe, R. Smith, The durability of clear polyurethane coil coatings studied by FTIR peak fi tting, Polym. Degrad. Stab. 98 (2013) 527–534.